

DESIGN AND IMPLEMENTATION OF AN INDUCTION FURNACE

Isam M. Abdulbaqi¹, Abdul-Hasan A. Kadhim², Ali H. Abdul-Jabbar³, Fathil A. Abood⁴, Turki K. Hasan⁵

¹ Professor, ^{2,3} Lecturer, ⁵ Assistant Professor / Elect. Eng. Dept. / College of Eng. / Al-Mustansiriya University

⁴ Lecturer / Elect. Eng. Dept. / College of Eng. / University of Babylon

E-mail: embaki56@yahoo.com¹, abdulhasan_abdulla@yahoo.com²,

alih_jabbar@yahoo.com.³ fathil_alhilli@yahoo.com⁴, turkihassan@yahoo.com⁵

(Received: 4/12/2012; Accepted: 2 /12/2013)

ABSTRACT: - The design of a certain induction furnace for a certain application depends mostly on empirical formulas and experience. The purpose of this work is to use the Finite Element Method (FEM) approach to perform an electromagnetic-thermal coupled analysis for a suggested coil with certain billet and studying its performance during the heating period. This will lead to the ability of expecting the required coil current and its frequency, to heat certain part of a certain billet to a certain temperature at the predetermined time. Then, the simulation results can be used to build the coil and leads to design the power supply for the induction furnace. The practical measurement of the designed system agrees with that of the theoretical design results. Hence, this approach assists to reduce the design cost, time and efforts for any other required induction furnace.

Keywords: Induction heating, Induction furnace, Finite Element Method (FEM).

LIST OF SYMBOLS

Symbol	Description	Units
A	Magnetic Vector Potential	Wbm^{-1}
B	Magnetic Flux Density	Tesla
C_p	Specific Heat	$\text{kJ/kg}^\circ\text{C}$
E	Electric Field	NC^{-1}
H	Magnetic Intensity	Am^{-1}
J	Current Density	Am^{-2}
k	Thermal Conductivity	$\text{W/m}^\circ\text{C}$
$Q_{\text{induction}}$	Volume Energy Density	Jm^{-3}
T	Temperature	$^\circ\text{C}$
T_{air}	Ambient Temperature	$^\circ\text{C}$
T_c	Time period of one cycle	s
T_{curie}	Curie Temperature	$^\circ\text{C}$
T_e	Element Temperature	$^\circ\text{C}$

T_n	Nodal Temperature	°C
α	Film Coefficient	$W^{\circ}C^{-1}$
ϵ	Permittivity	Fm^{-1}
μ_{reff}	Effective Relative Permeability	
μ_{ri}	Incremental Relative Permeability	
ξ	Emissivity of the Surface	
ρ_e	Electrical Resistivity	$\Omega.m$
σ_e	Electrical Conductivity of the Medium	Sm^{-1}
σ_s	Stefan-Boltzmann Constant	$Wm^{-2}K^{-4}$

INTRODUCTION:

It is already known that the design of the induction furnace depends mainly on general calculations and on the experience. This makes the design costly, tedious, and a time consuming task. In this research, a suggested approach is considered to design an induction furnace coil and determines the features of its power supply, that is suitable to furnish the following requirements; "*Heating a required part of a certain billet shape to the required temperature in a required time interval*". The suggested approach analysis will lead to design the induction heating system including the induction coil and its power source by determining the following:

- 1- The suitable induction coil shape.
- 2- The required induction coil current.
- 3- The required frequency of the induction coil current.

The above last two results will make it easy for the power supply designer to decide his circuit parameters, so this approach will expect the induction furnace performance theoretically.

THEORETICAL BACKGROUND

i. Electromagnetic Analysis

It is already known that the complex electromagnetic equations can be greatly simplified based on magnetic vector potential A . All quantities related to the induction Joule heat can be achieved, based on the AC current, I , input to the induction coil. A can be expressed with Biot-Savart's law ⁽¹⁾:

$$A = \frac{\mu_o I}{4\pi} \int_s \frac{dl}{|r|} \dots\dots\dots (1)$$

The magnetic flux density B is defined as

$$B = \nabla \times A \dots\dots\dots (2)$$

From Faraday's law, the electric field intensity E and magnetic field intensity H are related by the following equations:

$$\nabla \times E = -\frac{\partial B}{\partial t} \dots\dots\dots (3)$$

$$H = B / \mu \dots\dots\dots (4)$$

Based on Ampere’s circuital law, the current density, J , induced in work piece is

$$J = \nabla \times H - \frac{\partial(\epsilon \cdot E)}{\partial t} \dots\dots\dots (5)$$

After a mathematical manipulation of the above formulas, the relationship between the magnetic vector potential, A and the induced current density, J becomes

$$J = \nabla \times \left(\frac{1}{\mu} \nabla \times A \right) + \sigma_e \frac{\partial A}{\partial t} \dots\dots\dots (6)$$

Finally, Joule heat generated from eddy currents is

$$Q_{induction} = \frac{J^2}{\sigma_e} \dots\dots\dots (7)$$

The parameters μ, ϵ, σ_e , are the magnetic permeability, permittivity, and electrical conductivity of the medium respectively. These properties are all temperature dependent, and this makes the electromagnetic analysis as a highly nonlinear problem.

ii. Effective Relative Permeability [μ_{ref}]

The calculation of [μ_{ref}], must be started from the standard $B-H$ Curve at the ambient temperature. To do so, a function used by Vasiliev [2] for determination of the incremental relative permeability as a function of both T and H used as follows:

$$\mu_{ri}(H, T) = 1 + (\mu_{ri}(H)_{T=0} - 1) \cdot [1 - (T / T_{curie})^2] \text{ When } T < 750^\circ\text{C} \dots\dots\dots (8)$$

And $\mu_{ri}(H, T) = 1$ When $T \geq 750^\circ\text{C}$

$\mu_{ri}(H, T)$: represents the incremental relative permeability for each (H) as a function of temperature T and field intensity H .

$\mu_{ri}(H)_{T=0}$: represents the incremental μ relative permeability for each (H) as a function of H at $T = 0^\circ\text{C}$.

Razzaq (3), provides the $B-H$ curve at room temperature for Steel C45 (SAE 1045) as a magnetization curve drawn to be as shown in Figure (1). Curie temperature for steel C45 is 750°C .

The incremental relative permeability μ_{ri} calculated from the given $B-H$ data at $T = 25^\circ\text{C}$ for certain value of H as $\mu_{ri}(H)_{T=0} = [(\Delta B / \Delta H) / \mu_o]$ and substituted in (9) for the required value of T the result will be $\mu_{ri}(T, H)$ for that value of H for the required temperature. Then ΔB for the required value of T can be determined since, $\Delta B_T = \mu_o * \mu_{ri}(H, T) * \Delta H$, then, by dividing the main $B-H$ curve for many steps and the

incremental relative permeability calculated for each step, a new $B-H$ curve for any value of T can be achieved sequentially for different temperatures for the carbon steel C45.

In order to avoid the nonlinearity of the magnetic characteristics during the transient analysis, Fathil ⁽⁴⁾ presents the idea of average permeability to achieve the effective relative permeability. This idea states that, because neither B nor (H) is sinusoidal, considering the case of B is sinusoidal only, while H will have a distorted shape due to $B-H$ non linearity the average permeability will be

$$\mu_{reff1} = \frac{1}{T_c} \int_0^T \frac{B_{max} \sin \omega t}{B_T(T)} dt \dots\dots\dots (9)$$

Where $H_B(t)$: represents the distorted time variation of the field intensity.

T_c : represents the time period of one cycle.

In the case of considering H is sinusoidal only, while B will have a distorted shape due to ($B-H$) non linearity the average permeability will be

$$\mu_{reff2} = \frac{1}{T} \int_0^T \frac{B_H(t)}{H_{max} \sin \omega t} dt \dots\dots\dots (10)$$

Considering $B_H(t)$, representing the distorted time variation of the flux density.

Since, in the real case B and H are non-sinusoidal; therefore averaging both permeabilities would be a reasonable approximation to the effective permeability, then

$$\mu_{reff} = (\mu_{reff1} + \mu_{reff2})/2 \dots\dots\dots (11)$$

Using (11), the effective relative permeability as a function of H and T can be determined. It is clear that Fathil's method deals carefully with low intensity region.

iii. Thermal Analysis

Thermal analysis includes conduction, convection and radiation. The heating process is coupled with the electromagnetic conversion process. In the heating process, the conduction equation is ⁽²⁾,

$$\rho_m \cdot C_p \cdot \frac{\partial T}{\partial t} = k \cdot \nabla^2 T + Q_{induction} \dots\dots\dots (12)$$

Where: $Q_{induction}$ is the Joule heat achieved from the electromagnetic process, which is known as HGEN in ANSYS terminology.

On the surfaces of work piece, the heat conduction, radiation and free convection effects are all needed. The governing equation is,

$$\rho_m C_p \frac{\partial T}{\partial t} = k \nabla^2 T + Q_{induction} - \xi \sigma_s (T^4 - T_{air}^4) - \alpha (T - T_{air}) \dots\dots\dots (13)$$

T_{air} : Represents the ambient temperature.

THE MODEL

The designed furnace in this research is no more than a laboratory prototype used to verify the proposed approach, so it is not designed for certain application. The longitudinal cross-section of the furnace coil and its core that considered as a cylindrical billet are shown in Fig. (2). Table (1) represents the dimensions of the furnace and the billet.

Electromagnetic-thermal coupled analysis on the model by using ANSYS 13 computer package. The electromagnetic analysis is a steady state analysis considers the nonlinear magnetizing characteristics of the Steel C45 billet, while the electromagnetic-thermal coupled analysis is a transient analysis considers the effective relative permeability. Both analyses are done using sinusoidal steady state coil current of 100A, and frequency of 50 kHz.

Figures (3, 4, and 5) represent the flux density, current density and joule heat distribution on the periphery surface through the points (a, b, c).

The flow chart shown in Figure (6) represents the algorithm used in the electromagnetic-thermal coupled analysis to study the transient behavior of the billet during the heating process, until the required temperature achieved, (Refer to Appendix-A for FEM modeling).

Figure (7) shows the transient analysis of the temperature versus time for the four nodes (a, b, c, d). The simulation results show that the highest temperature on the surface at node (d), which reaches 738.24°C after 13 minutes of operation as shown in Fig. (8).

THE FURNACE IMPLEMENTATION

The above results lead to design the single phase inverter to supply the required sinusoidal current with a frequency of 50 kHz. Integrated Gate Commutated Thyristors (IGCTs) ⁽⁶⁾ avoided in this research due to a low power prototype, while the half bridge inverter circuit designed to feed the induction furnace coil as shown in figure (9). Orcad 16.2 software package used to simulate the half-Bridge inverter to supply the furnace with the required current and frequency as shown in Figure (10). The expected voltage and current shown in Figures (11, 12) ^(7, 8).

THE PRACTICAL RESULTS

It is clear that the practical measurements agree with the simulated results, which means that the design approach do well. In spite of the absence of the application for this laboratory type furnace, but it gives an approval for the simulation procedure and encourages going forward in any other design.

This design implemented as shown in figure (13) and feeds the designed coil with 100A, 50 kHz during 13 minutes. The furnace coil shown in figure (14), during the heating process. The temperature measured with a thermal infrared camera. The simulation and practical temperature rise during the heating time curves shown in figure (15).

DISCUSSION

The achievement of this work is an algorithm aids in the design of an induction furnace for any application instead of the trial and error method, to avoid high costs and time consuming. It is found that the simulation of the heating process is too complicated due to the non-uniform distribution of the eddy current which leads to non-uniform heat distribution inside the billet. This non-uniform heat distribution leads to change the temperature dependent physical characteristics of the material are like; electrical resistivity $\rho_e(T)$, effective relative permeability $\mu_{r,eff}(H,T)$, thermal conductivity $\kappa(T)$. The measured results for the designed inverter and the designed induction coil of the induction heating system matched well with the simulation results. This means that this approach can be used to design any other required furnace easily and with lower cost as compared with the conventional method.

REFERENCES

- 1) J. Davies, and P. Simpson, (1979), "Induction Heating Handbook", McGraw-Hill Book Company (UK).
- 2) A. Vasiliev, I. Pozniak, V. Greshnov, (2003), "Modeling and Investigation Hardening Process", International Scientific Colloquium, Modeling for Electromagnetic Processing, Hannover, March (24- 26).
- 3) Razzaq A. Marsuq, (1994), "Analysis and Study of Design Criteria of Induction Furnaces", M.Sc. Thesis, University of Baghdad, Iraq. .
- 4) Fathil A. Abood, (2002), "Direct Circuit Coupled Based Finite Element Analysis of Three Phase Induction Motor", Ph.D. Thesis, University of Technology. Baghdad, Iraq.
- 5) Jorg Cstroeski, (2003), "Boundary Element Methods for Inductive Hardening", Ph.D. Thesis, University of Topenge, Germany.
- 6) R. Lürick, S. Bernet, M. Michel. (2008), "A new IGCT Converter Topology for High Power Induction Heating Converters", Applied Power Electronics Conference and Exposition (APEC), pp. 1879 - 1884.

- 7) Ovidiu Pop, Adrian Taut, (2010), “Analysis and Simulation of Power Inverter with Load Variation for Induction Heating Applications”, 33rd International Spring Seminar on Electronics Technology (ISSE), pp. 378 – 382.
- 8) Abdul-Hasan A. Kadhim, (2011), “Half Bridge Resonant Inverter”, Al-Qadissiyah Journal of Engineering Sciences, Vol. 4, No. 3, pp. 340-352.

Table (1): represents the dimensions of the furnace and the billet.

Part	Dimension	Material
No. of turns	11	Copper
External coil radius	50mm	
Internal coil radius	80mm	
Coil height	1100mm	
Billet radius	12.5mm	Steel C45
Billet height	100mm	

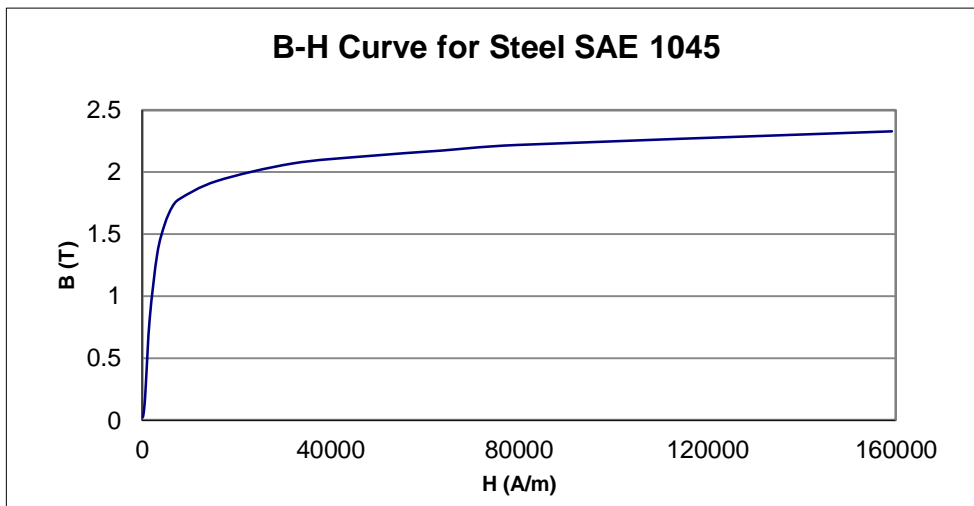


Figure: (1): The magnetization curve for steel C45 at room temperature.

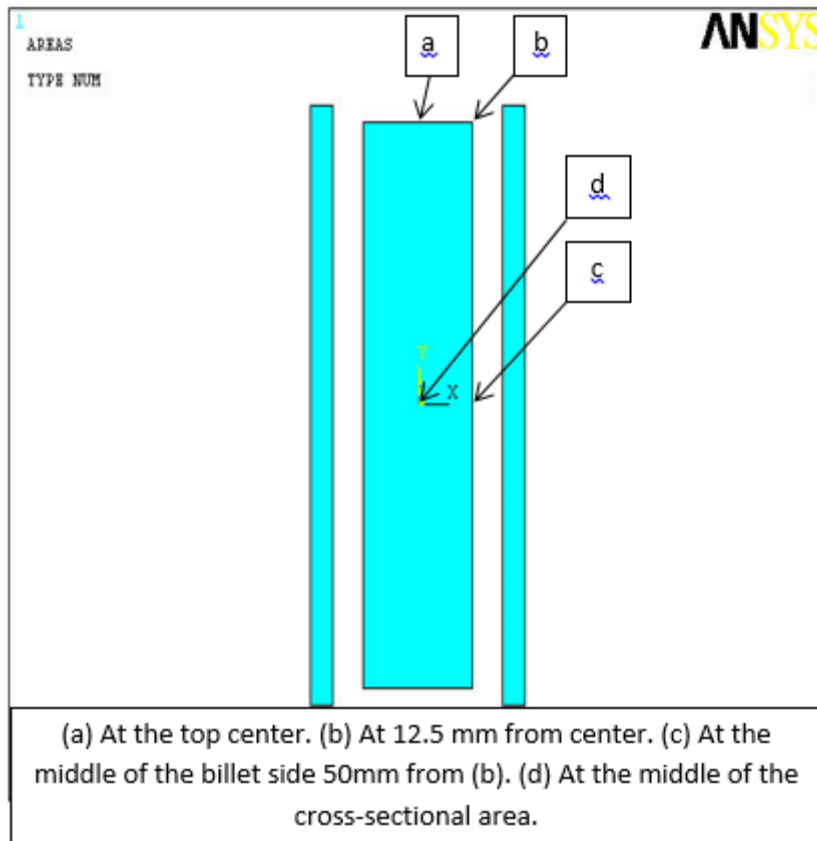


Figure (2): Longitudinal Cross-section for the billet and coil side.

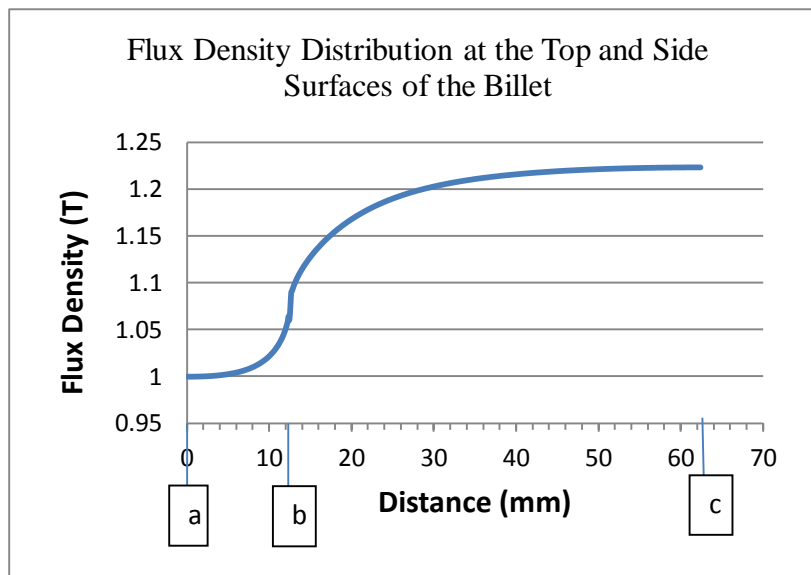


Figure: (3): the billet surface flux density distribution

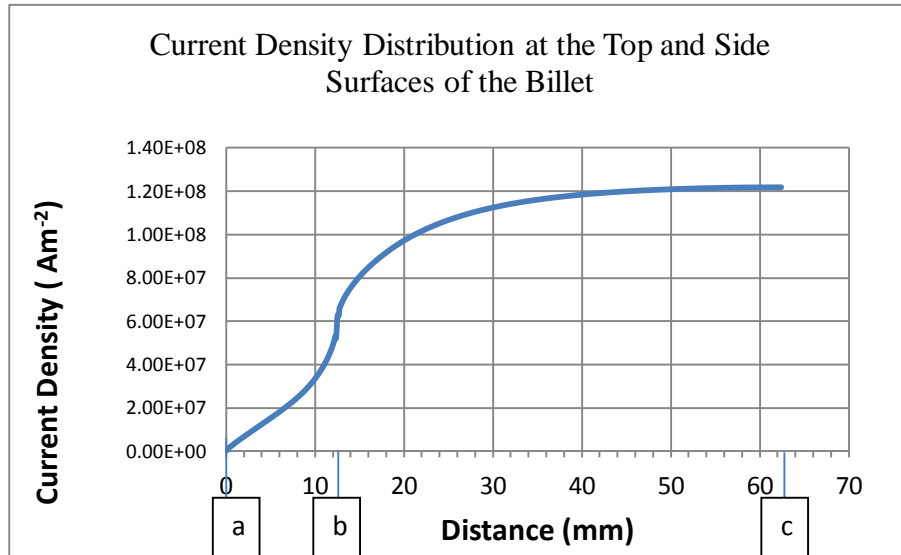


Figure (4): The billet surface eddy current density distribution.

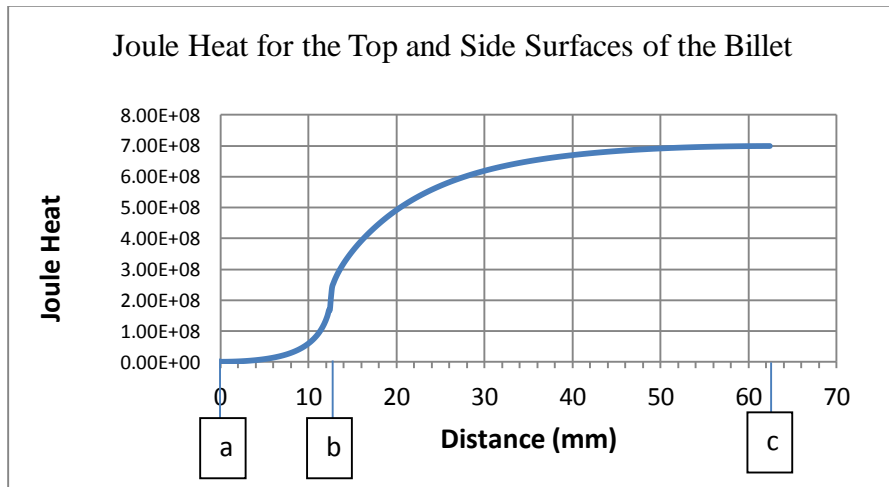


Figure: (5): The billet surface joule heat distribution

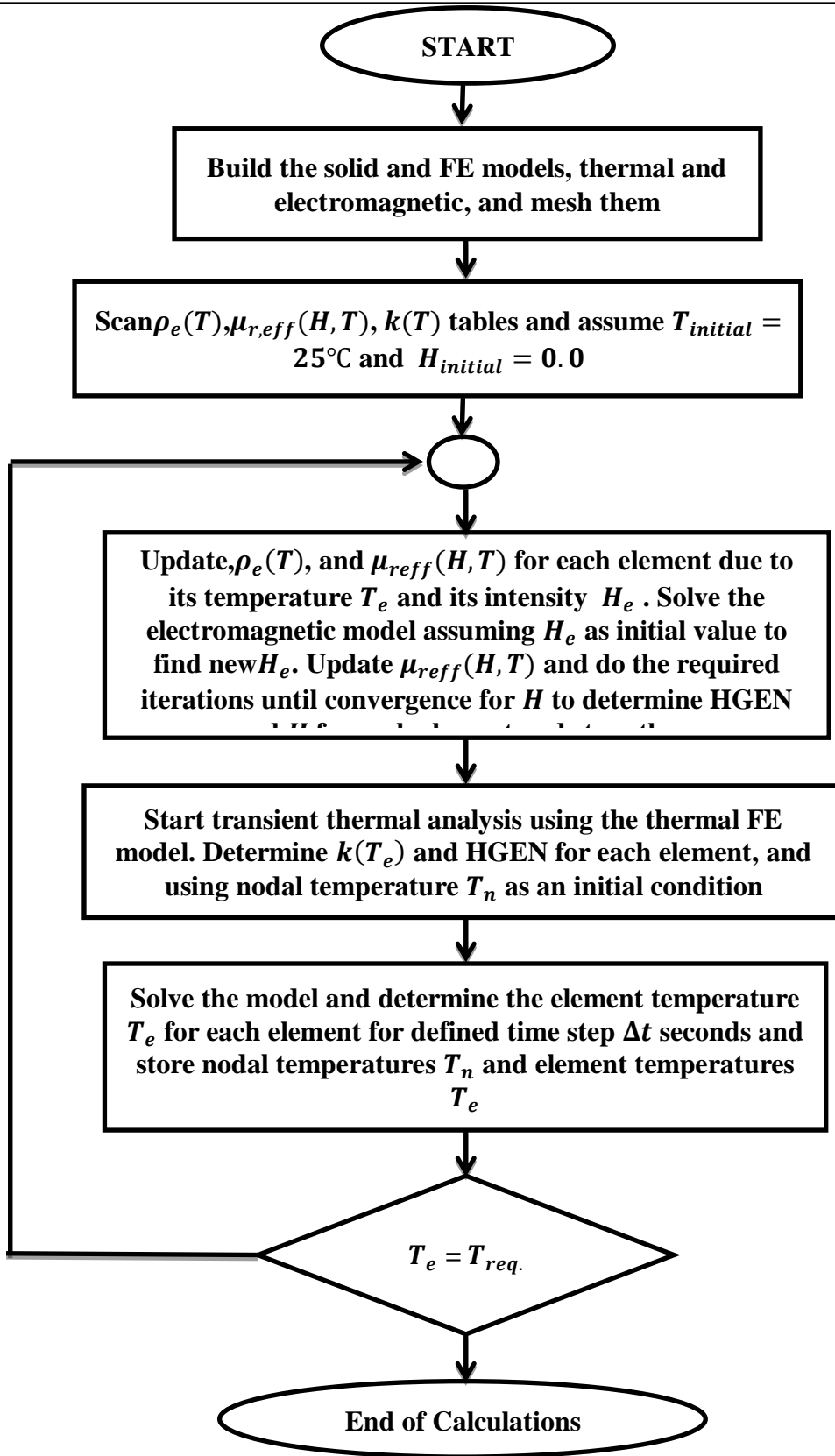


Figure: (6):.The flow chart of the heating process simulation.

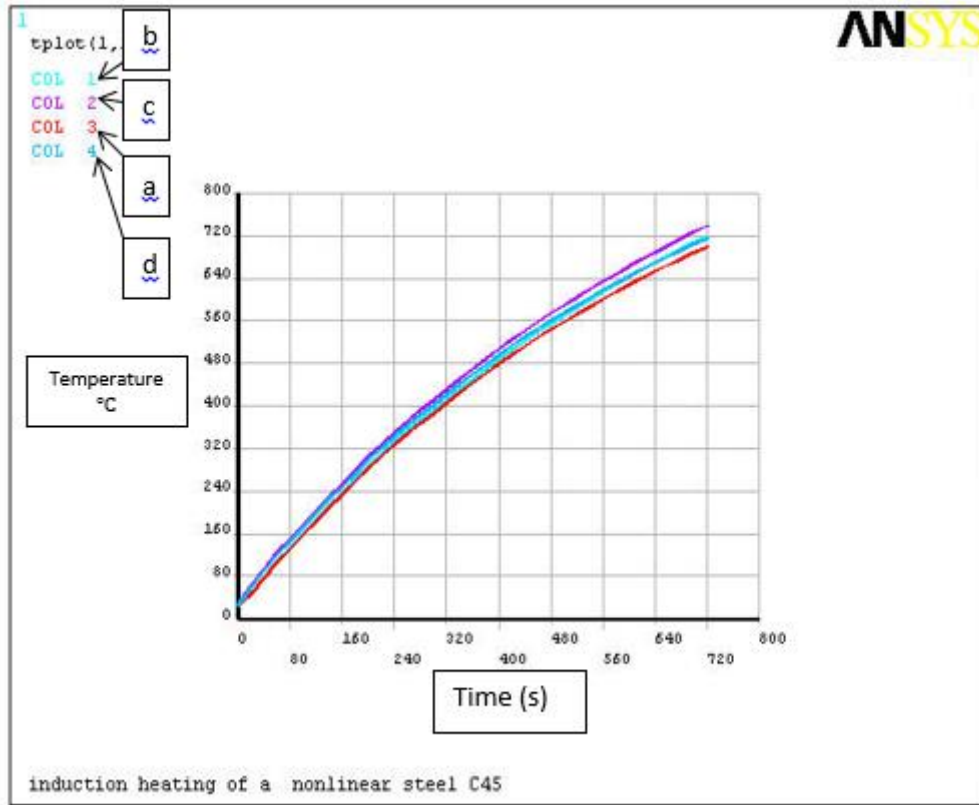


Figure: (7): The temperature rises during the heating process for the points a, b, c, and d

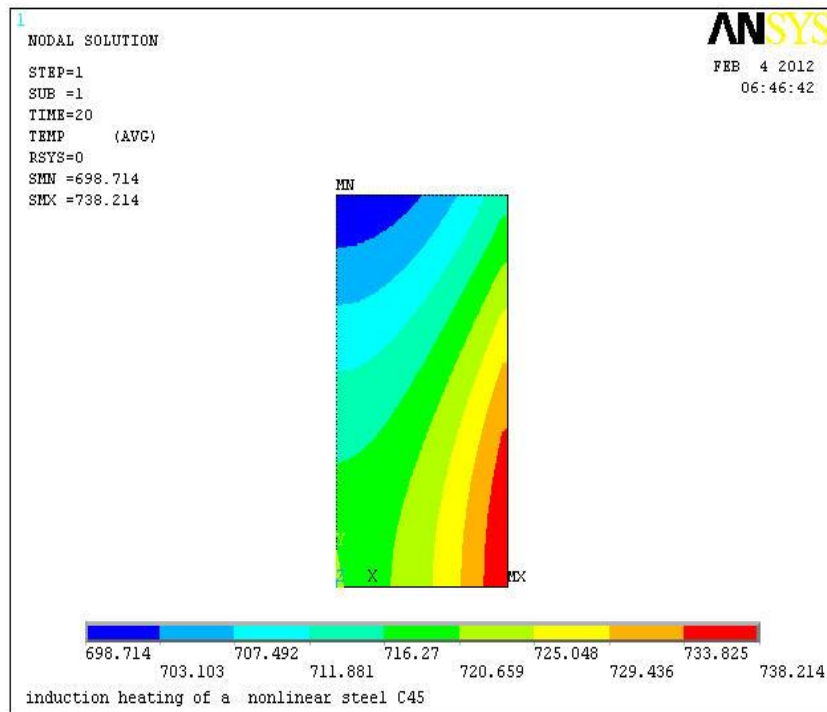


Figure: (8): The temperature distribution inside the billet

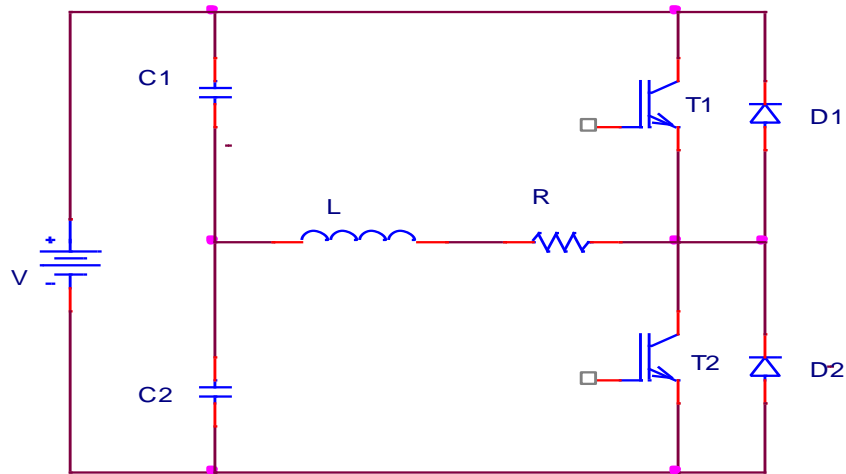


Figure (9): Half-Bridge inverter.

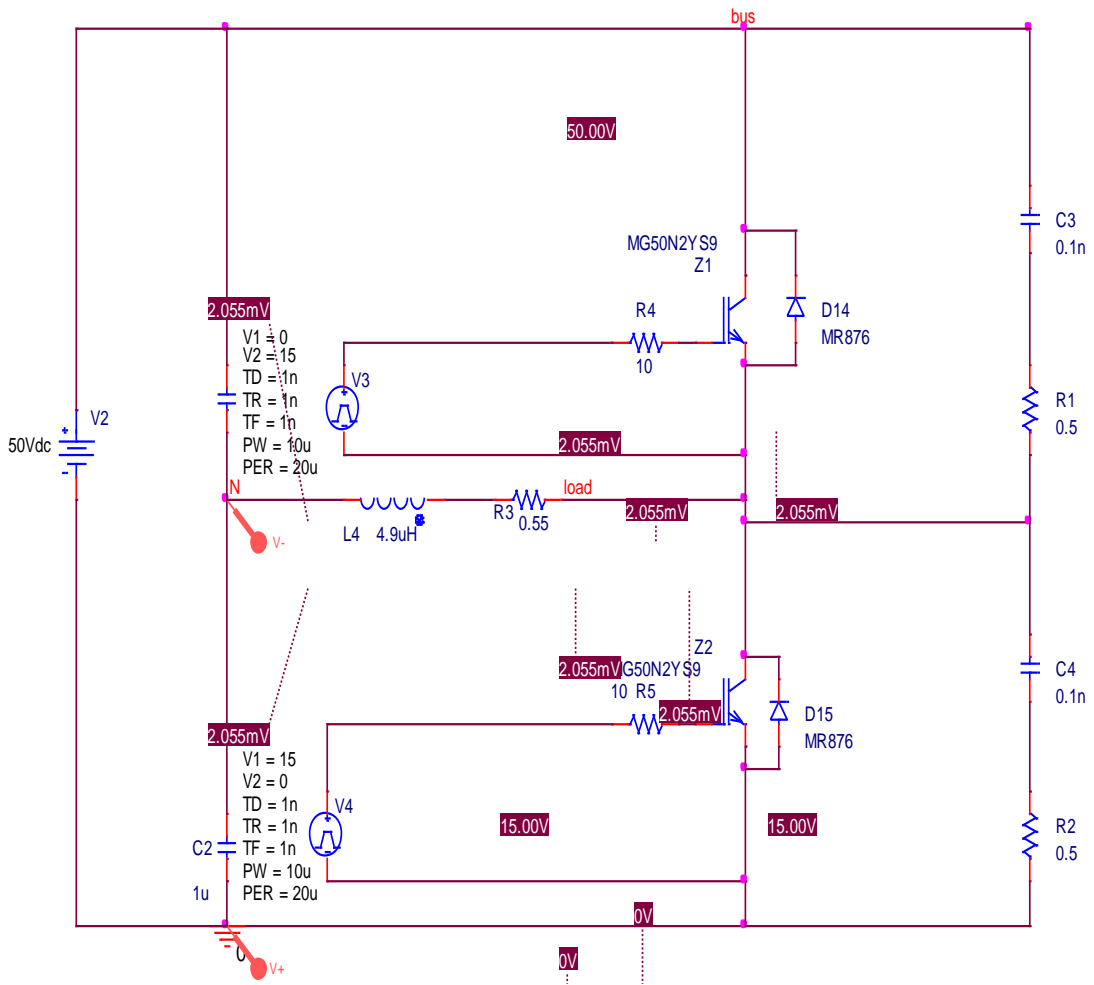


Figure (10): The simulated half-bridge inverter circuit

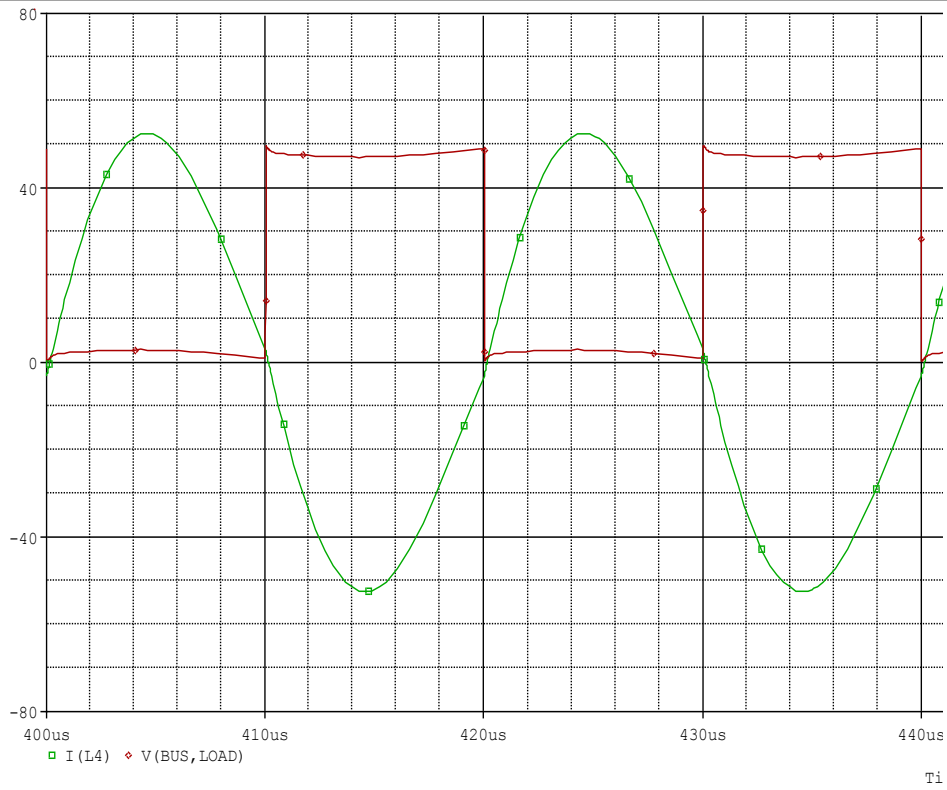


Figure (11): The load current (I_L) and collector-emitter (V_{CE}) versus time.

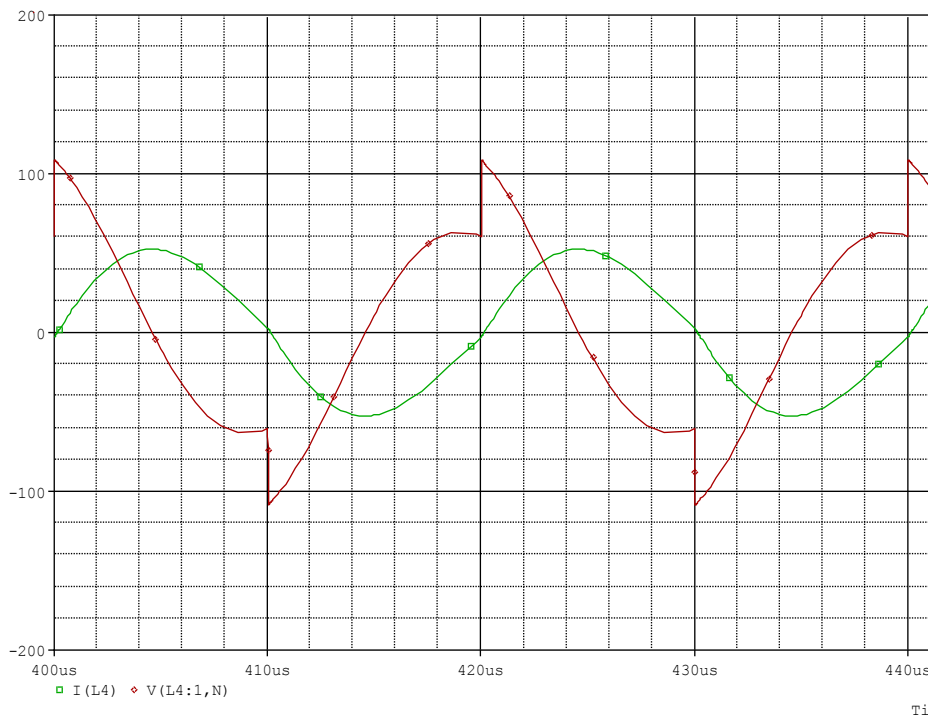


Figure (12): Load current (I_L) and load voltage (V_L) versus time.



Figure (13): The laboratory inverter circuit.



Figure (14): It represents the increase in billet temperature, during the heating process.

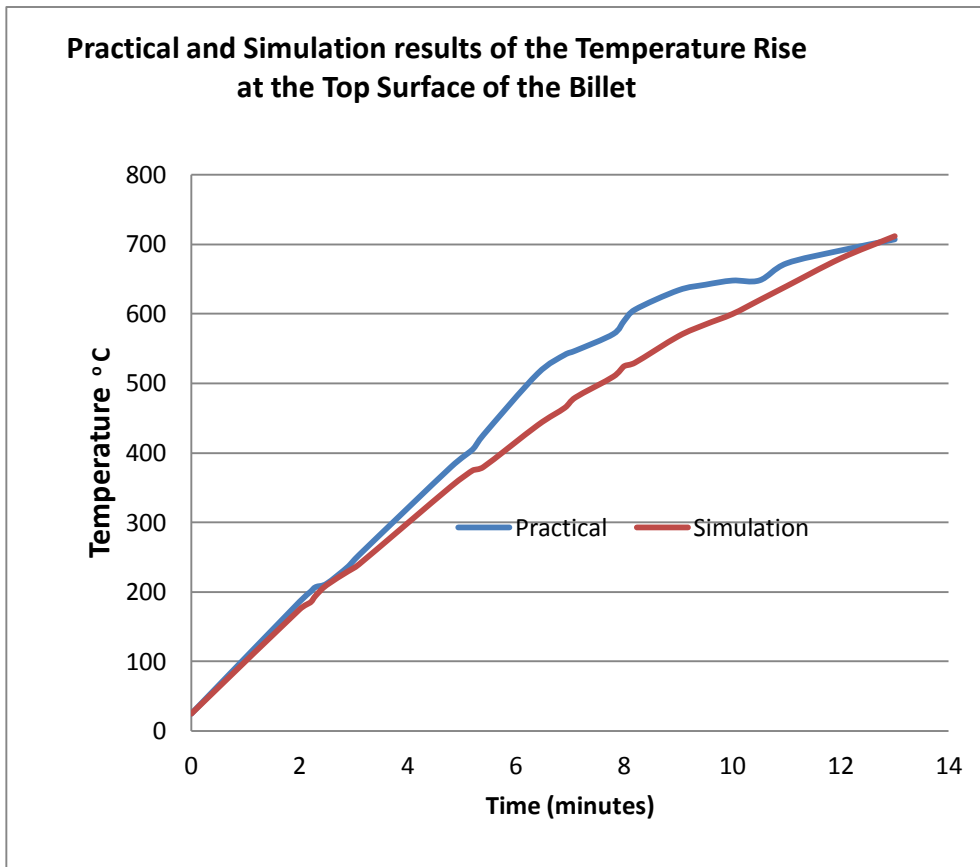


Figure (15): The theoretical and practical measurements of the top surface show the rise of temperature versus time during the heating process.

Appendix-A

The Modeling of Induction Furnace using FEM

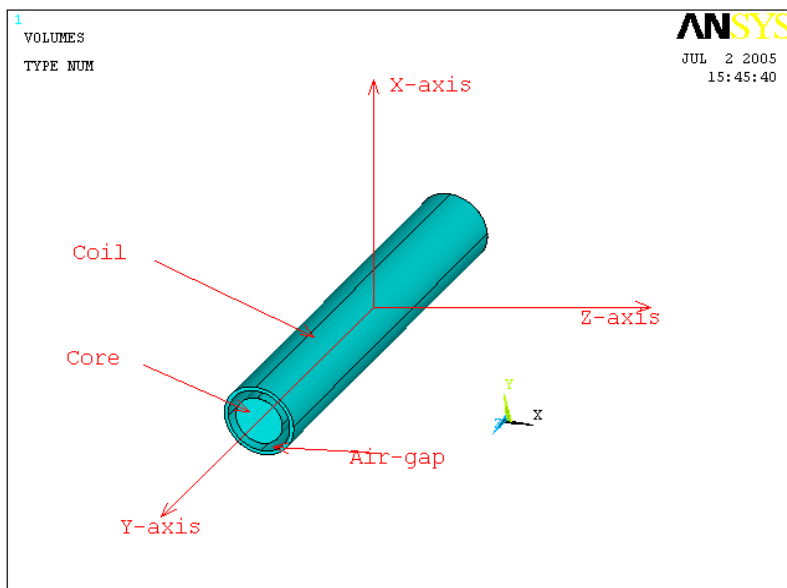


Figure (A-1): Orientation of the furnace due to the axes

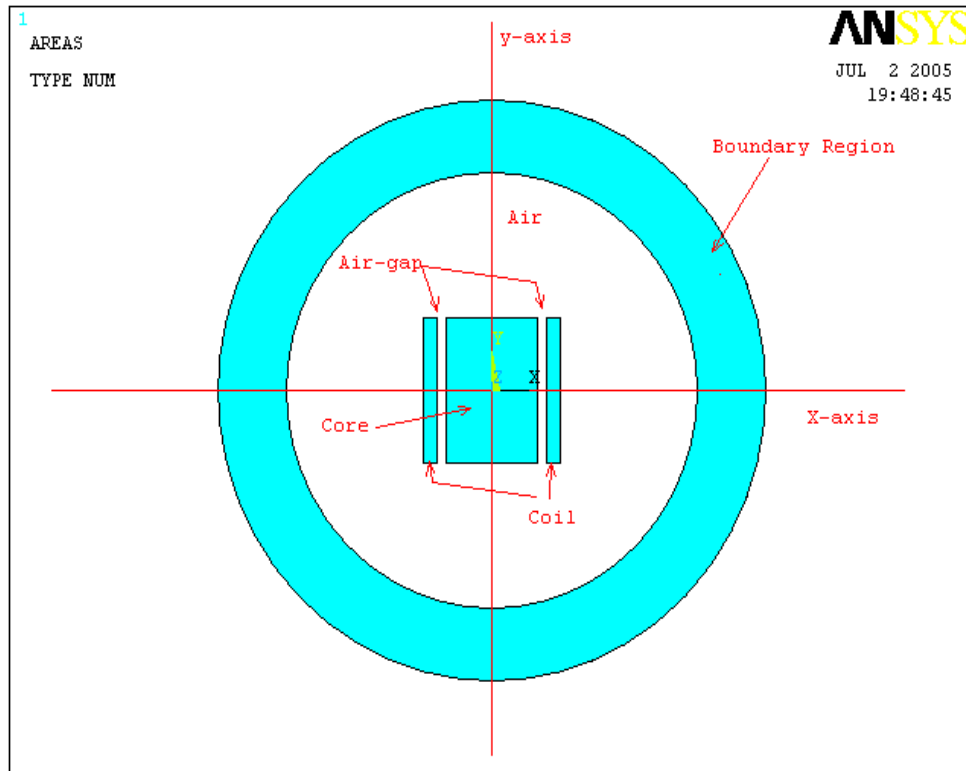


Figure (A-2): The x-y representation of the furnace with the boundary region.

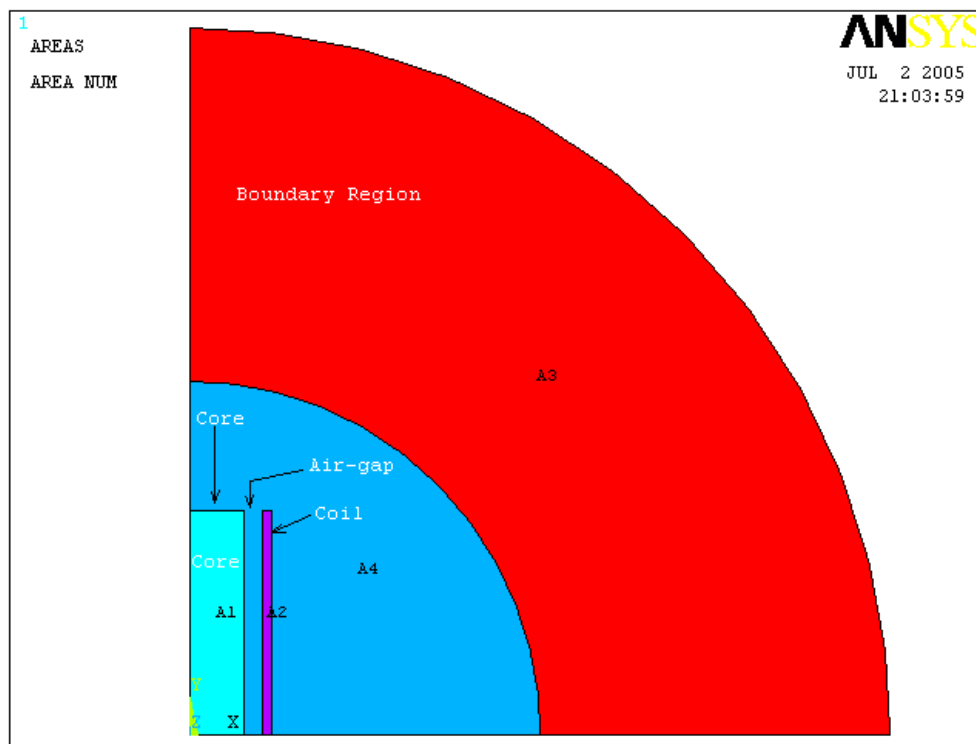


Figure (A-3): The section considered in calculations.

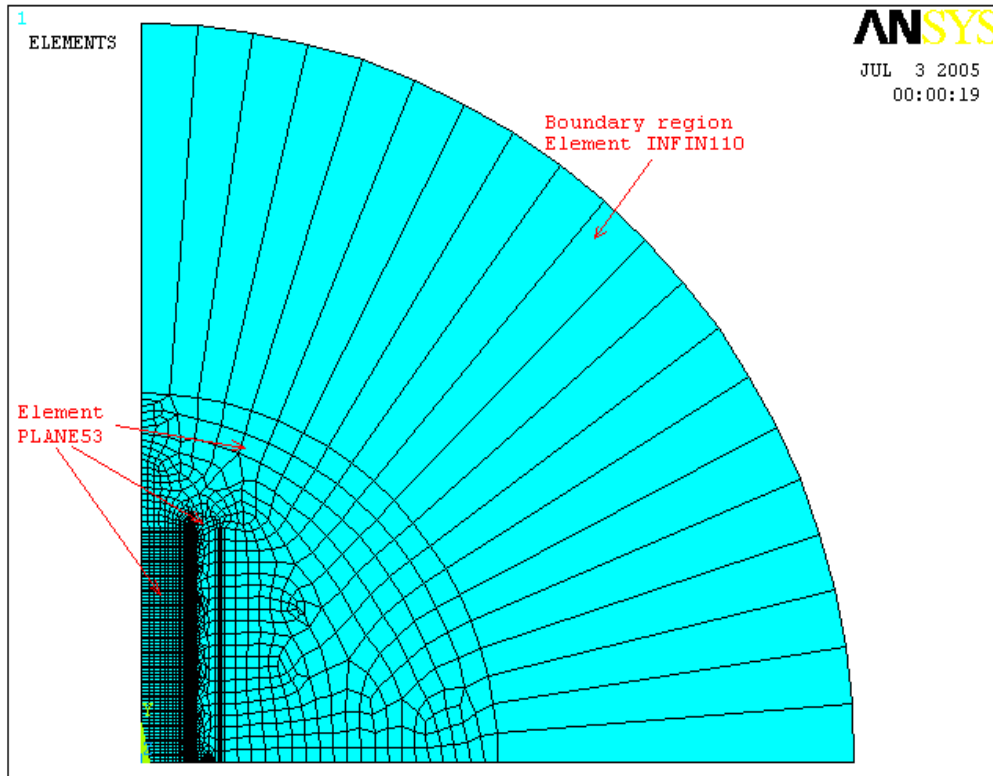


Figure (A-4): Mesh of the model by element PLANE53 and element INFIN110.

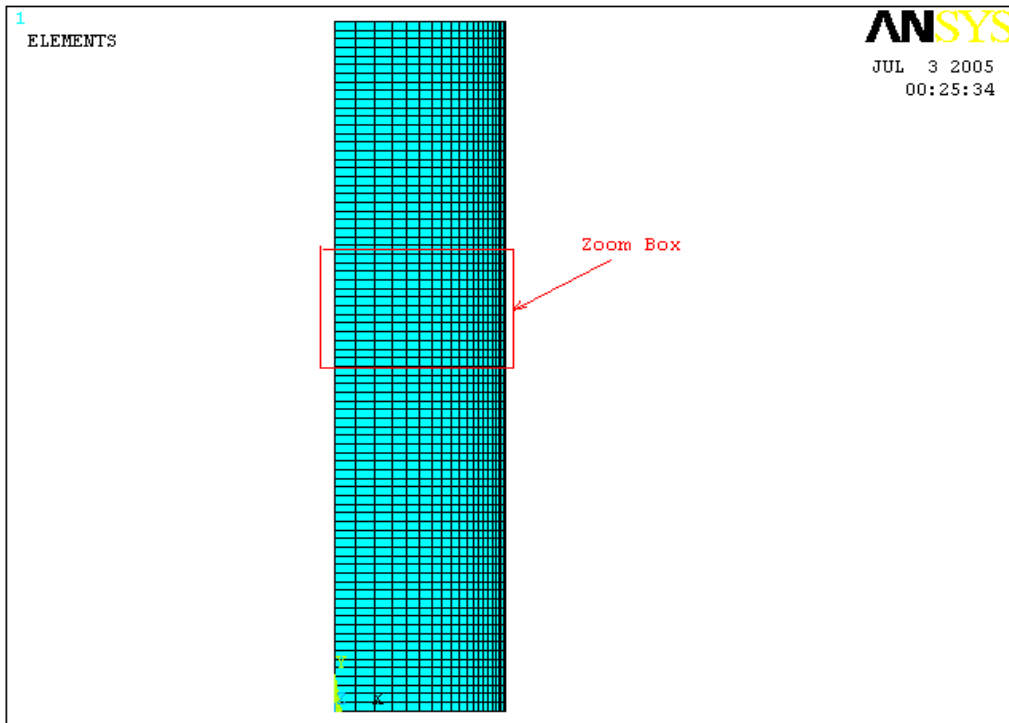
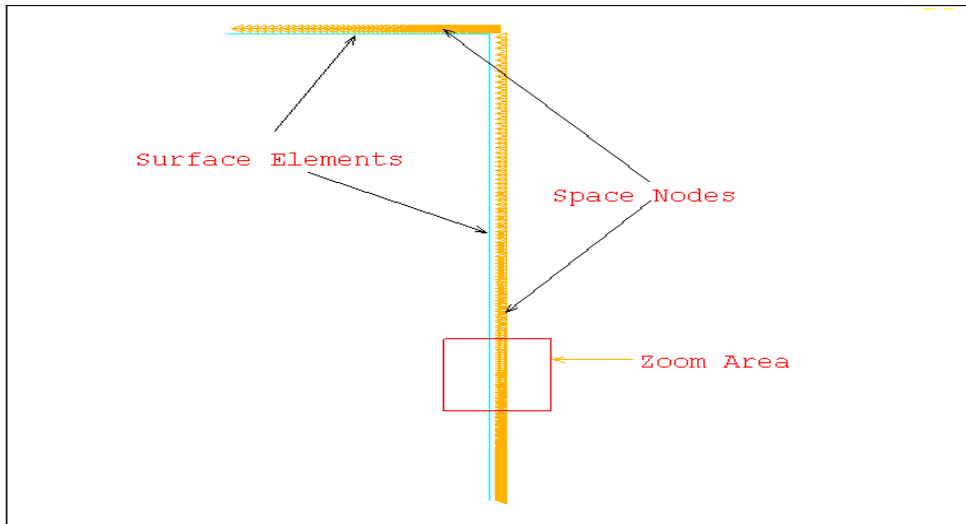
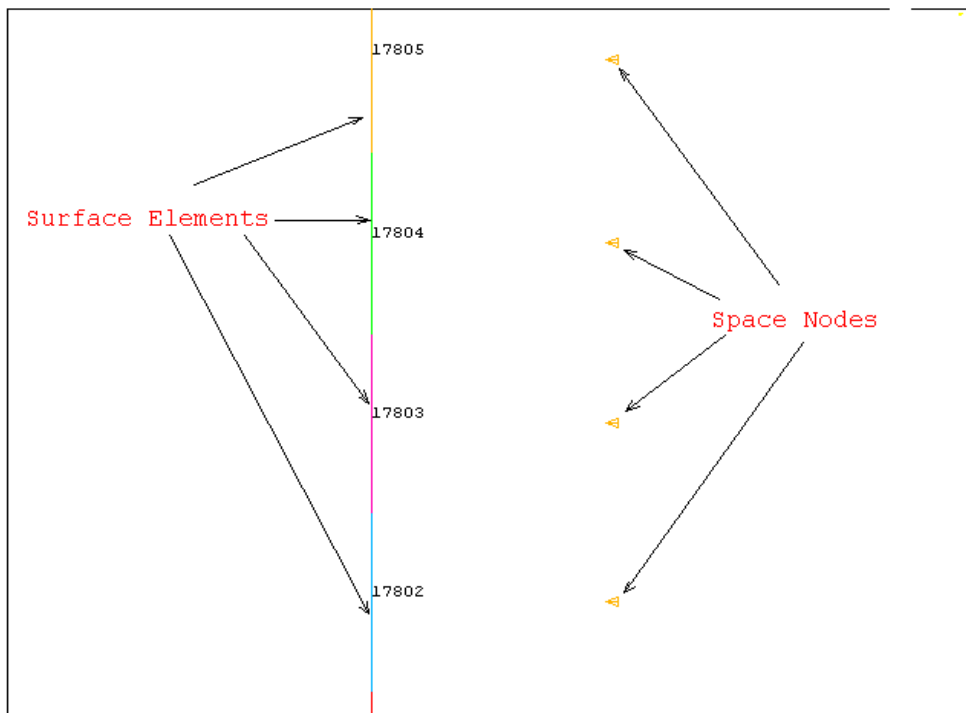


Figure (A-5): Meshing the billet such that the area of the elements very small near the surface in order to increase the accuracy of the electromagnetic analysis

Note: Thermal analysis done using the above mesh, but the elements replaced by PLANE55 which has the ability to measure the temperature distribution inside the core due to HGEN. While to measure the radiated energy due to emission and that due to convection, surface element SURF151 used for this purpose as shown in figure (6-A) (a, b).



(a) Surface elements type SURF151 for thermal analysis



(b) Enlarged scale to show surface element and its nodes

Figure (A-6): (a, b) represents the surface element SURF151 which is composed of three nodes. Two nodes on the external surface of the billet to calculate the emission of radiated energy, while the third node in space to calculate the convection in space around the billet.

تصميم و تنفيذ فرن حثي

أ.د. عصام محمود عبد الباقي¹، م. عبد الحسن عبد الله كاظم²، م. علي حسين عبد الجبار³،
م.د. فاضل علوان عبود⁴، أ.م.د. تركي كحيوش حسن⁵
^{1,2,3,5} قسم الهندسة الكهربائية/ كلية الهندسة/ الجامعة المستنصرية
⁴ قسم الهندسة الكهربائية/ كلية الهندسة/ جامعة بابل

الخلاصة:

يعتمد تصميم فرن حثي لأنجاز غرض معين في الغالب على الخبرة و المعادلات التطبيقية. ألباية من هذا العمل هي استخدام أسلوب (طريقة العنصر المحدد) (FEM) لأنجاز التحليلات المغناطيسية المقرنة بالحرارية لملف مقترح لحشوة (عينة) معينة و دراسة أدائه خلال فترة التسخين. أن هذا سيؤدي الى اكساب القابلية على توقع تيار الملف و تردده المطلوبين لتسخين جزء معين من عينة معينة الى درجة حرارة معينة في فترة زمنية محددة مسبقا. من ثم، سيتمكننا استخدام نتائج التمثيل لبناء ملف الفرن و سترشدنا الى تصميم مجهز القدرة للفرن الحثي. أن النتائج العملية للمنظومة المصممة توافقت مع التصميم النظري. لذلك، فأن هذا الأسلوب يساعد لتقليل الوقت و الجهد و الكلفة لبناء أي فرن حثي آخر مطلوب.